

Implicit Kinodynamic Motion Retargeting for Human-to-humanoid Imitation Learning

Xingyu Chen¹, Hanyu Wu², Sikai Wu¹, Mingliang Zhou¹, Diyun Xiang¹, Haodong Zhang³

¹Xiaomi Robotics Lab, ²ETH Zurich, ³Zhejiang University

Abstract—Human-to-humanoid imitation learning aims to learn a humanoid whole-body controller from human motion. Motion retargeting is a crucial step in enabling robots to acquire reference trajectories when exploring locomotion skills. However, current methods focus on motion retargeting frame by frame, which lacks scalability. Could we directly convert large-scale human motion into robot-executable motion through a more efficient approach? To address this issue, we propose **Implicit Kinodynamic Motion Retargeting (IKMR)**, a novel efficient and scalable retargeting framework that considers both kinematics and dynamics. In kinematics, IKMR pretrains motion topology feature representation and a dual encoder-decoder architecture to learn a motion domain mapping. In dynamics, IKMR integrates imitation learning with the motion retargeting network to refine motion into physically feasible trajectories. After fine-tuning using the tracking results, IKMR can achieve large-scale physically feasible motion retargeting in real time, and a whole-body controller could be directly trained and deployed for tracking its retargeted trajectories. We conduct our experiments both in the simulator and the real robot on a full-size humanoid robot. Extensive experiments and evaluation results verify the effectiveness of our proposed framework.

I. INTRODUCTION

Achieving diverse motor skills on humanoid robots is a long-term goal for whole-body imitation learning [1]–[7]. However, due to the limitations of humanoid robot hardware assets, it is unrealistic to collect massive and diverse robot motion data from real humanoid robots [8], [9]. In contrast, human motion data is relatively easier to obtain than robotic motion data [10], [11]. Human motion can be acquired through motion capture systems [12]–[14], where actors wear a series of magnetic or optical sensors to sample their key body positions. In addition to optical motion capture, human motion can be extracted from a vast number of videos on the internet [15]–[18]. Moreover, motion with audio [19], text [20]–[22], object and scene [23], [24], fill the gap in multi-modal dataset. Recent years, by combining with generative models, synthetic motion data can be generated from collected human motion data through various diffusion models [25]–[28] and auto-regressive models [29]–[32]. Currently, substantial human data has great potential to compensate for the scarcity of humanoid data, making humanoid whole-body imitation learning based on diverse human data extremely promising, as depicted in Figure 1. Nevertheless, it lacks an efficient and scalable approach for translating these large amount of data into robotic form.

Given motion data from a skeleton, the objective of motion retargeting is to drive the source motion into the target skeleton [33], ensuring that the character’s movements after

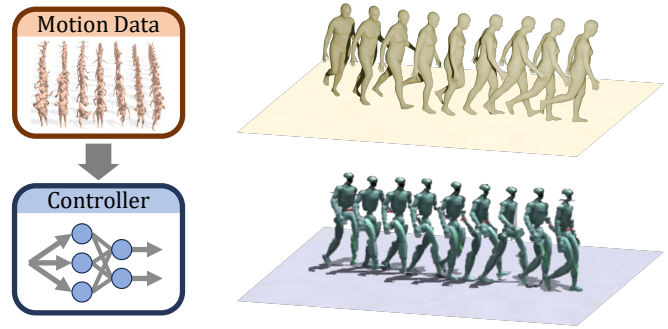


Fig. 1: **Human-to-humanoid imitation learning.** Given a reference human motion, a whole-body controller generates dynamically feasible actions for a humanoid robot, enabling it to achieve kinematically similar and diverse movements.

retargeting remain consistent with the source motion in terms of geometric and semantic features [34]. It is difficult for robots to learn directly from human data because the design of humanoid robots differs from that of real humans in terms of the number of joints and armatures, the length of bones and linkages. Therefore, current solutions usually abstract motion into sets of key points and model their relative relationships in space [35]–[38], then conduct a numeric optimization for each motion [39]. Some works apply post-processing to improve motion quality [40] and then utilize it for motion tracking. Kinematics-based approaches lack dynamic constraints [33], [41], often resulting in physically infeasible motions. While dynamics-based methods often involve manually designing physical constraints [42], they must balance numerical optimization precision against high computational costs. In addition to explicit motion retargeting, another method is implicit retargeting by a neural network. They extract latent space features [43] from motion sequences and try to learn a domain mapping [44]–[46] for computational efficiency. However, these approaches focus on virtual avatars and do not consider the dynamic constraints, which makes it physically infeasible. Furthermore, teleoperation from humans to robots requires precise and real-time motion conversion to achieve tracking from human posture to robotic posture. In this paper, we combine the advantages of these two types of approaches, and propose a novel framework **Implicit Kinodynamic Motion Retargeting (IKMR)**, a scalable and real-time retargeting method for imitation learning, which translates human motion into robot-executable motion and allows whole-body controller to directly mimic a period of human motion.

To learn a unified topology representation between the human and humanoid robot, we apply a dual encoder-decoder architecture for retargeting human motions onto a humanoid robot. In kinematics-aware pretraining, we construct paired human and humanoid robot motion sequence, sample the trajectory along the temporal dimension and leverage a skeleton-based graph convolutional encoder for critical latent motion feature extraction. Then, we reconstruct the motion using a symmetric decoder. During training, we align the latent space between human and humanoid robot. During retargeting, we reserve the reconstruct encoder while exchanging the decoder. In dynamics-aware fine-tuning, we introduce a imitation tracker for learning a physically feasible trajectory in simulator, and then fine-tune the motion decoder. Given a human motion, we could train and deploy a whole-body controller to track its retargeting result directly. Extensive experiment results verify the capability of our proposed framework. To summarize, we introduce a novel retargeting approach Implicit kinodynamic Motion Retargeting (IKMR), the key contributions of our work are as follows:

- To address computation efficiency, we introduce an implicit retargeting method into the human-to-humanoid motion retargeting task. The neural network can process large-scale motion rapidly.
- For robustly processing diverse motion, we propose a kinematics-aware pretraining strategy, which aims to learn a human-to-humanoid motion mapping through a unified motion representation in terms of skeleton topology. That facilitates IKMR able to deal with diverse motion against noise.
- To improve motion quality, we propose a dynamics-aware fine-tuning strategy in IKMR, which integrates imitation learning to utilize simulation data for post-training, enabling it to decode physically feasible motion.
- Our proposed approach is capable of translating large-scale human motion into robot-executable motion in real-time. We conduct extensive experiments on a full-size humanoid robot Unitree G1, and the results in simulation and real robot verify the capability of our proposed framework.

II. RELATED WORKS

A. Motion Retargeting

Early motion retargeting methods primarily focused on optimization with kinematic objectives and constraints [33], [41], treating it as a fitting problem of joint positions or link orientation between source and target skeletons. Then, the inverse kinematics method [47] reserves the end-effector positions and computes the joint angles to achieve higher precision. To preserve essential physical properties of the motion, some research proposes spacetime constraints dynamics [42] to maintain realism of the original motion. An intermediate skeleton [36] was explored to convert movements between hierarchically and geometrically different characters. For human-to-humanoid motion retargeting, current methods mainly employ a hierarchical process [39], [48],

Metrics	PHC [39]	Mink [48]	GMR [49]	IKMR (Ours)
Type	numeric	numeric	numeric	network
Constraint	FK	IK	IK	FK+dynamic
Speed	21fps	49fps	64fps	5000fps
Real-time	×	✓	✓	✓
Scalable	×	×	×	✓

TABLE I: Comparison with current retargeting methods used in the task of whole-body control. We test the speed using Intel Core i7-14700HX, RTX 4090. Scalability indicates whether the method supports vectorization for parallel computing.

[49], first matching body scales, and then optimizing joint poses. These approaches often operate frame-by-frame, and require optimizing parameters for each trajectory.

B. Neural Motion Processing

With the development of deep learning, the neural network performs a low-cost and high-efficiency approach to learn the motion mapping. The primary learning-based retargeting work [50] employs a convolutional neural network to reduce the temporal dimension of the motion sequence, while it ignores the topology structure of the character skeleton. To address this problem, researchers begin to model the character skeleton as a graph [51], where nodes and edges express joints and bones, respectively. Then, the convolutional kernel could be applied on the joint and its neighbors [52]. Inspired by the CycleGAN [53], researchers begin to introduce this architecture in the motion retargeting task, and develop it to an unsupervised paradigm [44], [45]. Given the target skeleton, pose2motion [46] learn a pose prior that transfers source motion without target motion in the training dataset. Recently, a dynamic graph transformation module [54] is proposed to handle unseen skeletal structures for humanoid motion retargeting.

C. Humanoid Imitation Learning

DeepMimic [55] pioneers imitation learning for humanoid characters by deep reinforcement learning. It directly applies the tracking error as a reward to encourage the agent to fit the trajectory. Then ASAP [56] proposed a delta action model to reduce the sim to real gap between simulator and real robot. KungfuBot [40] introduce an adaptive sigma for each reward function for high precision tracking. Also, some researches model the motion transition as a distribution, AMP [57] applies an adversarial network to provide a style reward for imitating the state transition. Early imitation learning methods usually train a policy to track one reference motion, ASE [58] develops a high-level controller for scheduling fundamental skills. To adapt for tele-operation, more advanced imitation methods have recently been proposed, such as OmniH2O [2], Exbody [3], HumanPlus [59], TWIST [1] and GMR [49]. However, current humanoid whole-body control strategies mainly apply explicit motion retargeting. In this paper, we introduce implicit retargeting into humanoid imitation learning.

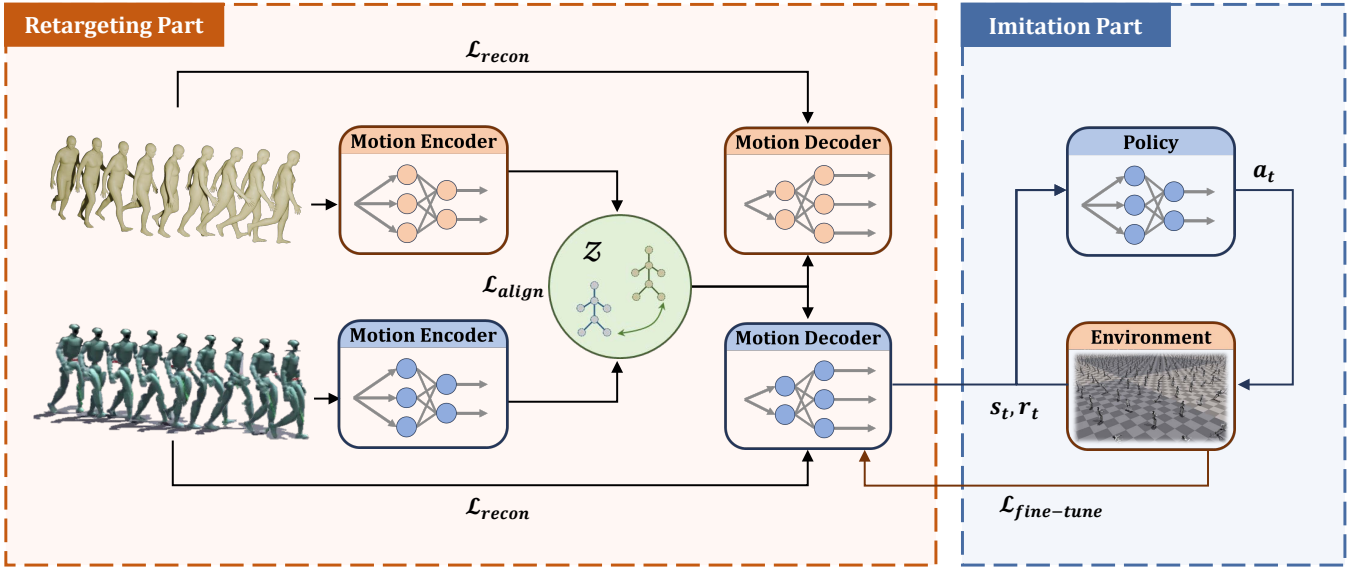


Fig. 2: Overall pipeline for our proposed framework. We model motion retargeting as a sequence-to-sequence mapping from source to target skeleton. In pre-training, we take a dual reconstruction and align the latent space. During retargeting, we reserve the encoder while exchanging the decoder. In post-training, we train an imitation tracker for learning a robot-executable motion in the simulator, then fine-tune the motion decoder to make it output physically feasible motion.

III. PROPOSED METHOD

A. Problem Formulation

In general, the motion representation consists of two components: a static part that describes the physical structure, and a dynamic part that expresses the state over time. For the static branch, it contains a relation skeleton tree and an initial skeleton state. The skeleton tree illustrates the hierarchical structure of a digital human skeleton, specifying the connections and movement relationships between joints and links through nodes and edges. The agent skeleton is defined as $S \in \mathbb{R}^{J \times S}$, where J is the number of joints, and S is the dimension of the static offset features. It describes joint offsets when the skeleton is in a particular initial pose.

For the dynamic branch, it contains a sequence of root translation and joint rotation. The root translation presents the position of the root node in the global coordinate system over time frames. The joint rotation is defined as $Q \in \mathbb{R}^{T \times J \times Q}$, it describes the joint state usually by local rotation in each time frame, where T is the length of frames, J is the number of joints, Q is the dimension of the dynamic features. In our setting, we use 3D vectors to represent static offsets, and use unit quaternions to represent local rotation from its parent's coordinate frame in the kinematic chain.

The problem of learning-based motion retargeting is defined using the following setup. Given a set of source motion $M_A = (S_A, Q_A)$ and the target motion $M_B = (S_B, Q_B)$ in pairs. We consider a training dataset $\mathcal{D} = \{(M_A^i, M_B^i)\}_{i=1}^n$, where each tuple comprises a human motion and a paired robot motion. Similar to the supervised learning paradigm, the implicit retargeting approaches aim to learn a functional mapping that predicts the target Q_B^i associated with source Q_A^i when the skeleton is predetermined, mathematically denoted as $f : Q_A \rightarrow Q_B$.

B. IKMR Network Architecture

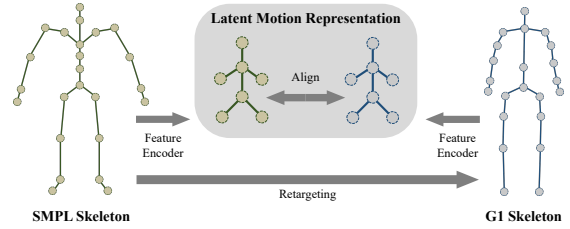


Fig. 3: Latent motion feature alignment between the human and humanoid robot. IKMR encodes motion from different structures into the shared representation space.

For human-to-humanoid motion retargeting, a basic assumption is that the source skeleton S_A and target skeleton S_B are homeomorphic (All limbs are connected to the torso), which means they are equivalent topologically in the kinematic chain, while they have many differences in skeletal structure, degree of freedom, and joint limitation. This will result in different locomotion performances between humans and humanoid robots when taking the same actions and behaviors, as well as significant trajectory gaps at the end effectors. For this reason, the retargeting process can suffer from inherent bias. Consider this, we abandon directly fitting joint angles and positions, instead we seek consistency at the feature level before and after retargeting. Specifically, given the input skeleton structure, each motion period could be extracted as latent motion features. Since the human and humanoid robots share the same topology chain, they could be compressed into the same set of topological prototypes shown in Figure.3, even if the number and length of joints are different. Once given a set of motion sequence pairs, the paired motion feature can be acquired through topology encoding. One of the target functions is to align the human and humanoid latent feature space.

C. Kinematics-aware Pretraining

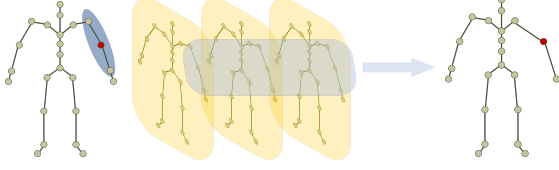


Fig. 4: Skeleton-based graph convolution and pooling. The motion encoder applies it to exact the spatial-temporal latent features for each joint and its neighbor in terms of the skeleton topology structure.

To extract the spatial-temporal latent motion features according to the skeleton topology, IKMR employs skeleton-based graph convolution and pooling layers as Figure.4. For each joint, its motion feature \hat{M} is calculated as

$$\hat{M}_i = \Phi(M_i) = \frac{1}{|N_i|} \sum_{j \in N_i} ((Q_j^i \odot S_j^i) * W_j^i) + b_j \quad (1)$$

where $M_i \in \mathbb{R}^{T \times (Q+S)}$ represents the i -th joint's feature, the kernel Φ is parameterized by weight $W_i \in \mathbb{R}^{T \times (Q+S) \times K}$ and bias $b_i \in \mathbb{R}^{T \times (Q+S) \times K}$, where K is the number of learned filters. Adjacency lists N_i is the neighbor set of i -th joint. The skeleton-based graph convolution layer traverses each joint, with all topologically adjacent joints participating in the computation. After that, the average pooling will be employed via

$$\text{Pooling}\{\hat{M}_i\} = \frac{1}{|N_i|} \sum_{j \in N_i} \hat{M}_j^i \quad (2)$$

For the network architecture, we follow the previous works [45] using a symmetric dual autoencoder. Each encoder-decoder contains a static block and a dynamic block. In the static block, it only operates the skeleton offset S . For the dynamic block, it concatenates static feature and then takes convolution in the whole motion as Figure.5.

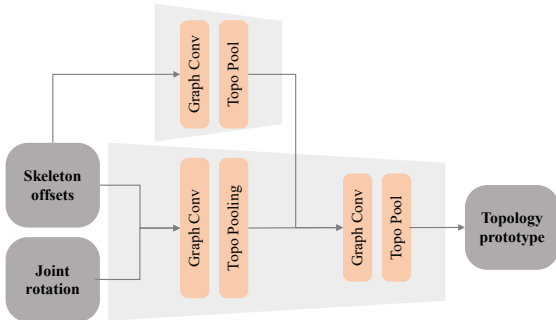


Fig. 5: Layer structure in motion encoder, it contains the static branch and the dynamic branch. With the graph convolution and pooling, source skeleton and motion will be compressed into topology motion representation.

We denote the reconstruction as $\hat{Q}_A = \mathbf{D}_\phi^A(z_A, S_A)$ and $\hat{Q}_B = \mathbf{D}_\phi^B(z_B, S_B)$, where the latent features are $z_A = \mathbf{E}_\theta^A(Q_A, S_A)$ and $z_B = \mathbf{E}_\theta^A(Q_B, S_B)$. The retargeting process is formulated as $\hat{Q}_B = \mathbf{D}_\phi^B(\mathbf{E}_\theta^A(Q_A, S_A), S_B)$, which uses the source motion encoder and target motion

decoder. In the pretraining stage, the main loss term is calculated as follow

$$\mathcal{L}_{align} = E_{(S_A, Q_A^i) \sim M_A} \left\| \mathbf{E}_\theta^A(Q_A, S_A) - \mathbf{E}_\theta^A(Q_B, S_B) \right\|^2 \quad (3)$$

Topology alignment loss. It is the core term for leading motion encoders to learn a unified representation between both the human side and humanoid robot side. This is the key condition enabling the subsequent exchange of decoders for retargeting.

$$\mathcal{L}_{recon} = E_{(S_A, Q_A^i) \sim M_A} \left[\left\| \mathbf{D}_\phi^A(\mathbf{E}_\theta^A(Q_A, S_A), S_A) - Q_A^i \right\|^2 \right] + E_{(S_B, Q_B^i) \sim M_B} \left[\left\| \mathbf{D}_\phi^A(\mathbf{E}_\theta^B(Q_B, S_B), S_A) - Q_A^i \right\|^2 \right] \quad (4)$$

Reconstruction loss. It is the main term for learning a compress encoding such that the original motion and paired retargeted motion can be recovered.

$$\mathcal{L}_{consis} = E_{(S_A, Q_A^i) \sim M_A} \left\| \mathbf{E}_\theta^A(\hat{Q}_A, S_A) - \mathbf{E}_\theta^A(Q_A, S_A) \right\|^2 \quad (5)$$

Latent consistency loss. It is a regularization term to ensure that the encoded retargeted motion and its paired motion remain consistent. Thus, the objective function for pretraining combines these loss terms together:

$$\mathcal{L}_{pretrain} = \mathcal{L}_{recon} + \lambda_{align} \mathcal{L}_{align} + \lambda_{consis} \mathcal{L}_{consis} \quad (6)$$

D. Dynamics-aware Fine-Tuning

After retargeting, we tracking the pretrained trajectory as a standard reinforcement learning paradigm, where the robot applies a optimal policy p_θ to interact with simulator such that the cumulative expected reward $J(\theta)$ can be maximized.

$$J(\theta) = \mathbb{E}_{\tau \sim p_\theta(\tau)} \left[\sum_{t=0}^T \gamma^t r_t \right] \quad (7)$$

We train several policies including walking, running, kicking and upper body movements, and the main reward term is the joint position function

$$r_t = \exp \left(- \frac{\|q_t - \hat{q}_t\|_2^2}{\sigma_{jpos}} \right) \quad (8)$$

where q_t and \hat{q}_t is the target position and current position from rolling out transitions. For stability, we also apply the position limits, collision termination and torque penalty. Once the policy can perform well, then we deploy them in the simulator in order to collect the physically feasible motion. According to the simulated motion with dynamic constraints, we only use the robot side autoencoder, freeze the motion encoder, and then fine-tune the decoder. We introduce an end-effectors loss in order to learn precise contact positions for feets and hands.

$$\mathcal{L}_{ee} = E \left[\left\| FK(\mathbf{D}_\phi^B(\mathbf{E}_\theta^A(Q_A, S_A), S_B)) - FK(\hat{Q}_B) \right\|^2 \right] \quad (9)$$

The objective function for fine-tuning is following:

$$\mathcal{L}_{fine-tune} = \mathcal{L}_{recon} + \lambda_{ee} \mathcal{L}_{ee} \quad (10)$$

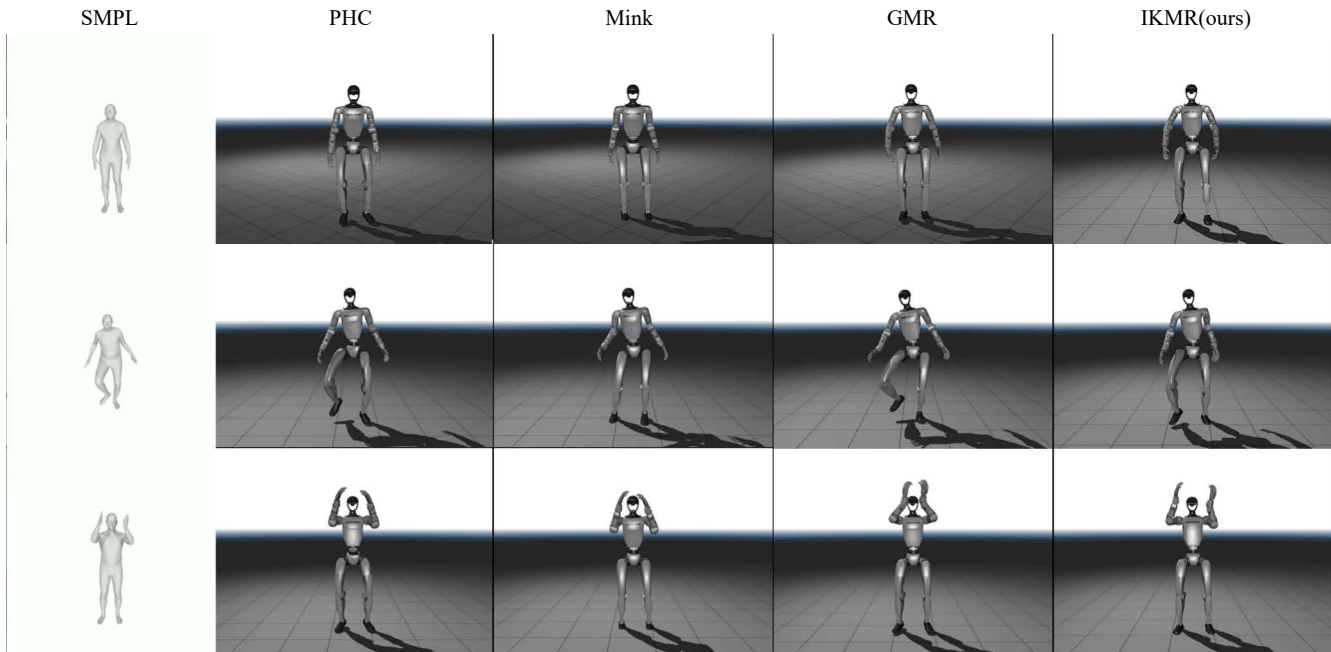


Fig. 6: Visualization of key frames of common methods PHC [39], Mink [48], GMR [49] and IKMR(ours) in human-to-humanoid imitation learning. The left one is the source human motion in SMPL format [60]. And the others are the retargeting motion in humanoid robot G1 format. Our proposed method can achieve diverse motion retargeting trajectories through feature encoding and decoding.

IV. EXPERIMENT

In kinematics-aware pretraining, our model is trained on the 2200 human-humanoid trajectory pairs, which sampling human data from AMASS dataset [61], and a rough retargeting by joint mapping. In dynamics-aware fine-tuning, we train six policy to sampling 440 physical feasible motion in simulator including walking, running, kicking and upper movement. To evaluate our retargeting results, We conduct our experiments on a full-size humanoid robot Unitree G1 with 132cm height, 35kg weight, and 29 degree of freedom to validate our retargeting approach both in simulation and real world.

A. Topology feature analysis

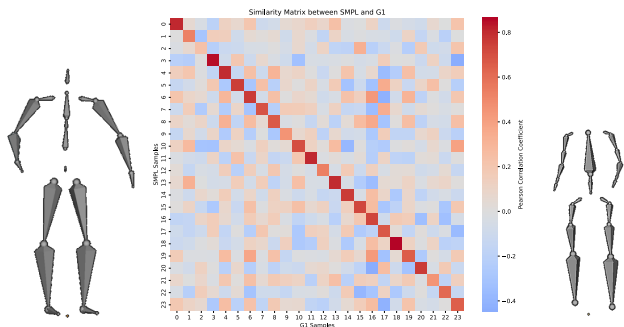


Fig. 7: Correlation matrix of latent features. We sample 24 paired trajectories from different types of motion, and obtain topology feature through the motion encoder. Then the similarity of the each topology features is calculated using Pearson correlation.

To perform a quantitative analysis of our unified topology representation, we select 24 different paired motion clips and

employ the Pearson correlation coefficient as the similarity to measure the distance between two latent space encoded vectors. The results in Figure.7 show that our model align well on the topology feature between human motion and humanoid motion. In the similarity matrix, the max correlation coefficient is 0.8638, it indicates feature alignment is lossy, resulting in incomplete transfer of motion features across the skeleton due to inherent differences in physical structures. The mean correlation coefficient is 0.0195, It is close to zero and presents the latent space exhibits uniform distribution without clustering in any specific region. Our unified topological motion representation effectively distinguishes different motion pattern, resulting in higher similarity between paired motion encoding and lower similarity between unpaired motion encoding.

B. Dynamics-aware fine-tuning

Although kinematic retargeting exhibit low error in static position fitting, their motion contains numerous physically unreasonable phenomena. Our dynamics-aware fine-tuning effectively mitigates these physical errors, producing smooth motion trajectories. To validate this, we introduced the acceleration and jerk metric to compare trajectories before and after fine-tuning. Acceleration measures the change rate of angular velocity, while jerk calculates the change rate of acceleration. Jerk reflects the force change rate in motion, representing smoothness of movement and coordination.

We conduct a comparison experiment between pre-train motion and fine-tuning motion in Table.II. We randomly samples 2,400 corresponding motion clips from the pre-train and fine-tuning retargeting motion to calculate the average acceleration and jerk per joint. Results indicate that when

inputting the same human reference trajectory, fine-tuned retargeting motions typically perform a lower acceleration and jerk values per joints, enabling more skilled and human-like movements.

	<i>Mean Acc</i> ↓	<i>Mean Jerk</i> ↓
pre-train	30.20 rad/s^2	456.60 rad/s^3
fine-tune	29.15 rad/s^2	435.37 rad/s^3

TABLE II: Comparison of motion smoothness.

By fine-tuning our network using dynamics constrained motion data, the decoder learns practical robot trajectories based on the features of the topology. When performing the same action, the fine-tuned trajectory enables execution with lower acceleration compared to the pre-trained motion, resulting in smoother and more coordinated movement. This approach ensures the stability of the robot while preserving the characteristics of the source data. Through experimental comparison, unrealistic movements such as model penetration, slipping, and floating that existed in the pre-trained network have been significantly mitigated.

C. Comparison experiment

We select some key frames in the retargeting motion and visualize it in Figure.6, it illustrates the final appearance of our retargeting trajectory compared with PHC [39], Mink [48], GMR [49], three common methods used in whole-body control. In terms of computational efficiency, we test above retargeting approaches in Intel Core i7-14700HX, RTX 4090. Our method achieves 5000 fps retargeting speed, nearly 100 times faster than numerical optimization techniques for one motion trajectory retargeting shown in Table.I. Furthermore, our approach has ability to scale across batch dimensions, enabling parallel computation of multiple trajectories for dataset-level retargeting.

To consider practically characteristics, this section focuses on the robustness of retargeting methods to noisy data. Because, in video motion capture and motion generation, the source human motion data often contains noise. One advantage of implicit retargeting is its robustness to the noise from source data. Since the encoder extracts motion features implicitly, which facilitates IKMR able to deal with diverse motion against disturbance. We evaluate the impact on retargeting results by adding noise artificially to the source motion data and progressively increasing the noise’s proportional coefficient level. The evaluation metrics are as follows:

- *Absolute Keypoints Trajectory Error.*

Original ATE refers to the absolute error between the camera pose trajectory and the estimated camera pose trajectory in SLAM system. We introduce into our motion retargeting task, to measure the accuracy and consistency between the clean human motion and retargeting motion from noisy source. We select key joints contain the root, ankle, wrist, and knee. Lower AKTE indicates more accurate with ground truth.

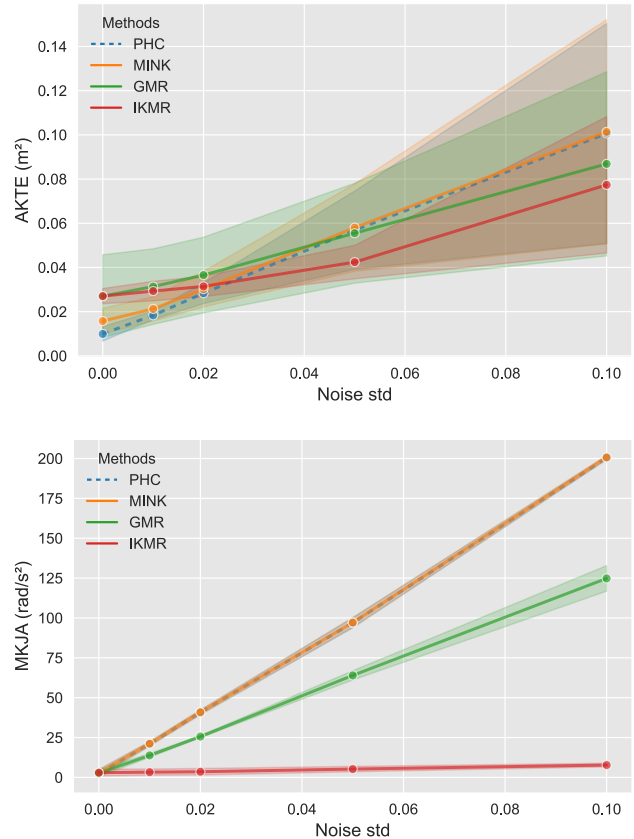


Fig. 8: Comparison of motion precision metric (a) Absolute Keypoints Trajectory Error and smoothness metric (b) Mean Key Joints Acceleration under different noise levels. Our proposed method IKMR maintains lower metric values with the noise increasing, indicating the robustness of our method against source motion noise conditions.

- *Mean Key Joints Acceleration.*

Mean Key Joints Acceleration refers to the average linear acceleration of the robot’s key joints, including the root, ankle, wrist, and knee. Lower AKJA generally indicates smoother movement.

To perform the evaluation, we inject zero-mean Gaussian noise with increasing standard deviation into the root translation of the source human motion and retargeted the motion to the G1 shown in Figure.8. With the noise level increasing, our method shows significantly robust performance in terms of keypoints trajectory and key joints acceleration. Numerical methods tend to fit motion noise, resulting in sudden large local accelerations, whereas neural network-based methods can mitigate local tremors caused by noise to a certain extent. This indicates that our approach can generate relatively smooth and stable robot motion in the presence of disturbances in the source motion, such as jitters. Experimental results demonstrate that our method achieves comparable performance to optimization-based methods in terms of keypoints trajectory error and key joints angular acceleration. This tolerance for noise significantly enhances the safety of the motor, making it promising for real-time video motion capture and teleoperation.

D. Imitation learning in robot

We test the our retargeting results in full-size humanoid robot G1. Given a human motion, a whole-body controller could be directly trained and deployed for tracking our retargeting trajectory. We selected several movements covering the upper and lower limbs with different directions:

- swinging arms for the upper body movement
- rapid leg kick for the lower body movement
- step forward with a human-like gait
- quickly running backward in a leaning-back posture

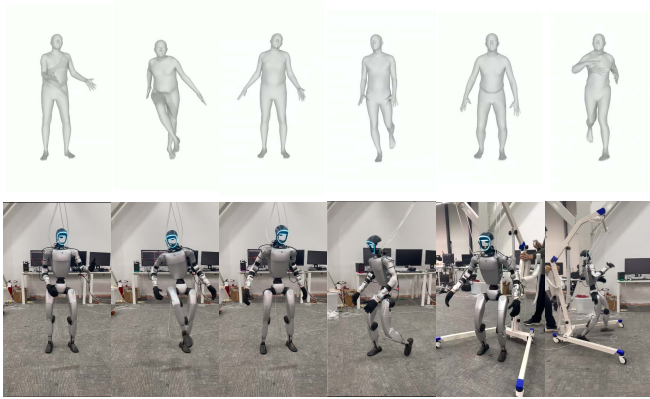


Fig. 9: Human-to-humanoid motion imitation in real robot.

Our implicit retargeting method enables downstream controllers to accurately capture and learn the details of human-like gait style, such as hip rotation and hip sway during forward walking, and backward lean during backward running. We validate the reliability of our retargeting results on actual devices through these representative movement. Our retargeting network provides an end-to-end approach enabling direct conversion of human motion data into humanoid robotic data. This method enables the tracker to reproduce the original motion with a high degree of accuracy.

V. CONCLUSION

In this paper, we propose Implicit Kinodynamic Motion Retargeting (IKMR), a novel real-time and scalable framework that considers both kinematics and dynamics motion retargeting. For limitation, our model can only convert sequences of a fixed length. For longer sequence, It must be split into sub-sequences and then reassembled. This results in discontinuities at the connection between sub-sequence output, leading to certain abrupt changes. For future work, we present the advantages of the proposed method in computational efficiency, motion quality, and noise robustness through extensive experiments. For topology latent space, it is promising to encode more robotics into unified representation. And network-based retargeting methods demonstrate a significant potential to bridge the gap between multimodal generative models and physics-based imitation learning.

REFERENCES

[1] Y. Ze, Z. Chen, J. P. Araújo, Z. ang Cao, X. B. Peng, J. Wu, and C. K. Liu, "Twist: Teleoperated whole-body imitation system," *arXiv preprint arXiv:2505.02833*, 2025. 1, 2

[2] T. He, Z. Luo, X. He, W. Xiao, C. Zhang, W. Zhang, K. Kitani, C. Liu, and G. Shi, "Omnih2o: Universal and dexterous human-to-humanoid whole-body teleoperation and learning," *arXiv preprint arXiv:2406.08858*, 2024. 1, 2

[3] X. Cheng, Y. Ji, J. Chen, R. Yang, G. Yang, and X. Wang, "Expressive whole-body control for humanoid robots," *arXiv preprint arXiv:2402.16796*, 2024. 1, 2

[4] Y. Xue, W. Dong, M. Liu, W. Zhang, and J. Pang, "A unified and general humanoid whole-body controller for versatile locomotion," *arXiv preprint arXiv:2502.03206*, 2025. 1

[5] A. Allshire, H. Choi, J. Zhang, D. McAllister, A. Zhang, C. M. Kim, T. Darrell, P. Abbeel, J. Malik, and A. Kanazawa, "Visual imitation enables contextual humanoid control," *arXiv preprint arXiv:2505.03729*, 2025. 1

[6] K. Yin, W. Zeng, K. Fan, Z. Wang, Q. Zhang, Z. Tian, J. Wang, J. Pang, and W. Zhang, "Unitracker: Learning universal whole-body motion tracker for humanoid robots," *arXiv preprint arXiv:2507.07356*, 2025. 1

[7] Z. Chen, M. Ji, X. Cheng, X. Peng, X. B. Peng, and X. Wang, "Gmt: General motion tracking for humanoid whole-body control," *arXiv preprint arXiv:2506.14770*, 2025. 1

[8] N. Rotella, M. Bloesch, L. Righetti, and S. Schaal, "State estimation for a humanoid robot," in *2014 IEEE/RSJ International Conference on Intelligent Robots and Systems*. IEEE, 2014, pp. 952–958. 1

[9] S. Kuindersma, R. Deits, M. Fallon, A. Valenzuela, H. Dai, F. Permenter, T. Koolen, P. Marion, and R. Tedrake, "Optimization-based locomotion planning, estimation, and control design for the atlas humanoid robot," *Autonomous robots*, vol. 40, no. 3, pp. 429–455, 2016. 1

[10] J. Lin, A. Zeng, S. Lu, Y. Cai, R. Zhang, H. Wang, and L. Zhang, "Motion-x: A large-scale 3d expressive whole-body human motion dataset," *Advances in Neural Information Processing Systems*, vol. 36, pp. 25 268–25 280, 2023. 1

[11] Y. Wang, S. Zheng, B. Cao, Q. Wei, W. Zeng, Q. Jin, and Z. Lu, "Scaling large motion models with million-level human motions," *arXiv preprint arXiv:2410.03311*, 2024. 1

[12] A. Kirk, J. F. O'Brien, and D. A. Forsyth, "Skeletal parameter estimation from optical motion capture data," in *ACM SIGGRAPH 2004 Sketches*, 2004, p. 29. 1

[13] L. Mündermann, S. Corazza, and T. P. Andriacchi, "The evolution of methods for the capture of human movement leading to markerless motion capture for biomechanical applications," *Journal of neuroengineering and rehabilitation*, vol. 3, no. 1, p. 6, 2006. 1

[14] M. Menolotto, D.-S. Komaris, S. Tedesco, B. O'Flynn, and M. Walsh, "Motion capture technology in industrial applications: A systematic review," *Sensors*, vol. 20, no. 19, p. 5687, 2020. 1

[15] Y. Wang, Z. Wang, L. Liu, and K. Daniilidis, "Tram: Global trajectory and motion of 3d humans from in-the-wild videos," in *European Conference on Computer Vision*. Springer, 2024, pp. 467–487. 1

[16] Z. Shen, H. Pi, Y. Xia, Z. Cen, S. Peng, Z. Hu, H. Bao, R. Hu, and X. Zhou, "World-grounded human motion recovery via gravity-view coordinates," in *SIGGRAPH Asia 2024 Conference Papers*, 2024, pp. 1–11. 1

[17] S. Shin, J. Kim, E. Halilaj, and M. J. Black, "Wham: Reconstructing world-grounded humans with accurate 3d motion," in *Proceedings of the IEEE/CVF Conference on Computer Vision and Pattern Recognition*, 2024, pp. 2070–2080. 1

[18] L. Müller, H. Choi, A. Zhang, B. Yi, J. Malik, and A. Kanazawa, "Reconstructing people, places, and cameras," in *Proceedings of the Computer Vision and Pattern Recognition Conference*, 2025, pp. 21 948–21 958. 1

[19] T. Tang, J. Jia, and H. Mao, "Dance with melody: An lstm-autoencoder approach to music-oriented dance synthesis," in *Proceedings of the 26th ACM international conference on Multimedia*, 2018, pp. 1598–1606. 1

[20] M. Plappert, C. Mandery, and T. Asfour, "The kit motion-language dataset," *Big data*, vol. 4, no. 4, pp. 236–252, 2016. 1

[21] C. Guo, S. Zou, X. Zuo, S. Wang, W. Ji, X. Li, and L. Cheng, "Generating diverse and natural 3d human motions from text," in *Proceedings of the IEEE/CVF Conference on Computer Vision and Pattern Recognition*, 2022, pp. 5152–5161. 1

[22] A. R. Punnakkal, A. Chandrasekaran, N. Athanasiou, A. Quiros-Ramirez, and M. J. Black, "Babel: Bodies, action and behavior with english labels," in *Proceedings of the IEEE/CVF conference on computer vision and pattern recognition*, 2021, pp. 722–731. 1

- [23] B. L. Bhatnagar, X. Xie, I. A. Petrov, C. Sminchisescu, C. Theobalt, and G. Pons-Moll, "Behave: Dataset and method for tracking human object interactions," in *Proceedings of the IEEE/CVF Conference on Computer Vision and Pattern Recognition*, 2022, pp. 15935–15946. [1](#)
- [24] Z. Wang, Y. Chen, T. Liu, Y. Zhu, W. Liang, and S. Huang, "Humanise: Language-conditioned human motion generation in 3d scenes," *Advances in Neural Information Processing Systems*, vol. 35, pp. 14959–14971, 2022. [1](#)
- [25] G. Tevet, S. Raab, B. Gordon, Y. Shafir, D. Cohen-or, and A. H. Bermano, "Human motion diffusion model," in *The Eleventh International Conference on Learning Representations*, 2023. [Online]. Available: <https://openreview.net/forum?id=SJ1kSyO2jwu> [1](#)
- [26] M. Zhang, Z. Cai, L. Pan, F. Hong, X. Guo, L. Yang, and Z. Liu, "Motiondiffuse: Text-driven human motion generation with diffusion model," *arXiv preprint arXiv:2208.15001*, 2022. [1](#)
- [27] C. Xin, B. Jiang, W. Liu, Z. Huang, B. Fu, T. Chen, J. Yu, and G. Yu, "Executing your commands via motion diffusion in latent space," in *Proceedings of the IEEE/CVF Conference on Computer Vision and Pattern Recognition (CVPR)*, June 2023. [1](#)
- [28] X. Chen, "Text-driven human motion generation with motion masked diffusion model," *arXiv preprint arXiv:2409.19686*, 2024. [1](#)
- [29] A. Ghosh, N. Cheema, C. Oguz, C. Theobalt, and P. Slusallek, "Synthesis of compositional animations from textual descriptions," in *Proceedings of the IEEE/CVF international conference on computer vision*, 2021, pp. 1396–1406. [1](#)
- [30] G. Tevet, B. Gordon, A. Hertz, A. H. Bermano, and D. Cohen-Or, "Motionclip: Exposing human motion generation to clip space," in *European Conference on Computer Vision*. Springer, 2022, pp. 358–374. [1](#)
- [31] J. Zhang, Y. Zhang, X. Cun, S. Huang, Y. Zhang, H. Zhao, H. Lu, and X. Shen, "T2m-gpt: Generating human motion from textual descriptions with discrete representations," in *Proceedings of the IEEE/CVF Conference on Computer Vision and Pattern Recognition (CVPR)*, June 2023. [1](#)
- [32] C. Guo, Y. Mu, M. G. Javed, S. Wang, and L. Cheng, "Momask: Generative masked modeling of 3d human motions," in *Proceedings of the IEEE/CVF Conference on Computer Vision and Pattern Recognition*, 2024, pp. 1900–1910. [1](#)
- [33] M. Gleicher, "Retargetting motion to new characters," in *Proceedings of the 25th annual conference on Computer graphics and interactive techniques*, 1998, pp. 33–42. [1](#), [2](#)
- [34] J. Zhang, J. Weng, D. Kang, F. Zhao, S. Huang, X. Zhe, L. Bao, Y. Shan, J. Wang, and Z. Tu, "Skinned motion retargeting with residual perception of motion semantics & geometry," in *Proceedings of the IEEE/CVF Conference on Computer Vision and Pattern Recognition*, 2023, pp. 13 864–13 872. [1](#)
- [35] K.-J. Choi and H.-S. Ko, "Online motion retargetting," *The Journal of Visualization and Computer Animation*, vol. 11, no. 5, pp. 223–235, 2000. [1](#)
- [36] J.-S. Monzani, P. Baerlocher, R. Boulic, and D. Thalmann, "Using an intermediate skeleton and inverse kinematics for motion retargeting," in *Computer Graphics Forum*, vol. 19, no. 3. Wiley Online Library, 2000, pp. 11–19. [1](#), [2](#)
- [37] K. Darvish, Y. Tirupachuri, G. Romualdi, L. Rapetti, D. Ferigo, F. J. A. Chavez, and D. Pucci, "Whole-body geometric retargeting for humanoid robots," in *2019 IEEE-RAS 19th International Conference on Humanoid Robots (Humanoids)*. IEEE, 2019, pp. 679–686. [1](#)
- [38] C. Schumacher, E. Knoop, and M. Bächer, "A versatile inverse kinematics formulation for retargeting motions onto robots with kinematic loops," *IEEE Robotics and Automation Letters*, vol. 6, no. 2, pp. 943–950, 2021. [1](#)
- [39] Z. Luo, J. Cao, K. Kitani, W. Xu *et al.*, "Perpetual humanoid control for real-time simulated avatars," in *Proceedings of the IEEE/CVF International Conference on Computer Vision*, 2023, pp. 10 895–10 904. [1](#), [2](#), [5](#), [6](#)
- [40] W. Xie, J. Han, J. Zheng, H. Li, X. Liu, J. Shi, W. Zhang, C. Bai, and X. Li, "Kungfubot: Physics-based humanoid whole-body control for learning highly-dynamic skills," *arXiv preprint arXiv:2506.12851*, 2025. [1](#), [2](#)
- [41] T. Tosun, R. Mead, and R. Stengel, "A general method for kinematic retargeting: Adapting poses between humans and robots," in *ASME international mechanical engineering congress and exposition*, vol. 46476. American Society of Mechanical Engineers, 2014, p. V04AT04A027. [1](#), [2](#)
- [42] Z. Popović and A. Witkin, "Physically based motion transformation," in *Proceedings of the 26th annual conference on Computer graphics and interactive techniques*, 1999, pp. 11–20. [1](#), [2](#)
- [43] S. Choi, M. K. Pan, and J. Kim, "Nonparametric motion retargeting for humanoid robots on shared latent space," in *Robotics: science and systems*, 2020. [1](#)
- [44] R. Villegas, J. Yang, D. Ceylan, and H. Lee, "Neural kinematic networks for unsupervised motion retargeting," in *Proceedings of the IEEE conference on computer vision and pattern recognition*, 2018, pp. 8639–8648. [1](#), [2](#)
- [45] K. Aberman, P. Li, D. Lischinski, O. Sorkine-Hornung, D. Cohen-Or, and B. Chen, "Skeleton-aware networks for deep motion retargeting," *ACM Transactions on Graphics (TOG)*, vol. 39, no. 4, pp. 62–1, 2020. [1](#), [2](#), [4](#)
- [46] Q. Zhao, P. Li, W. Yifan, S.-H. Olga, and G. Wetzstein, "Pose-to-motion: Cross-domain motion retargeting with pose prior," in *Computer Graphics Forum*, vol. 43, no. 8. Wiley Online Library, 2024, p. e15170. [1](#), [2](#)
- [47] J. Lee and S. Y. Shin, "A hierarchical approach to interactive motion editing for human-like figures," in *Proceedings of the 26th annual conference on Computer graphics and interactive techniques*, 1999, pp. 39–48. [2](#)
- [48] K. Zakka, "Mink: Python inverse kinematics based on mujoco, july 2024," URL <https://github.com/kevinzakka/mink>, vol. 10. [2](#), [5](#), [6](#)
- [49] Y. Ze, J. P. Araújo, J. Wu, and C. K. Liu, "Gmr: General motion retargeting," 2025, gitHub repository. [Online]. Available: <https://github.com/YanjieZe/GMR> [2](#), [5](#), [6](#)
- [50] D. Holden, J. Saito, and T. Komura, "A deep learning framework for character motion synthesis and editing," *ACM Transactions on Graphics (ToG)*, vol. 35, no. 4, pp. 1–11, 2016. [2](#)
- [51] S. Yan, Y. Xiong, and D. Lin, "Spatial temporal graph convolutional networks for skeleton-based action recognition," in *Proceedings of the AAAI conference on artificial intelligence*, vol. 32, no. 1, 2018. [2](#)
- [52] H. Ci, C. Wang, X. Ma, and Y. Wang, "Optimizing network structure for 3d human pose estimation," in *Proceedings of the IEEE/CVF international conference on computer vision*, 2019, pp. 2262–2271. [2](#)
- [53] J.-Y. Zhu, T. Park, P. Isola, and A. A. Efros, "Unpaired image-to-image translation using cycle-consistent adversarial networks," in *Proceedings of the IEEE international conference on computer vision*, 2017, pp. 2223–2232. [2](#)
- [54] H. Zhang, Z. Chen, H. Xu, L. Hao, X. Wu, S. Xu, R. Xiong, and Y. Wang, "Unified cross-structural motion retargeting for humanoid characters," *IEEE Transactions on Visualization and Computer Graphics*, 2024. [2](#)
- [55] X. B. Peng, P. Abbeel, S. Levine, and M. Van de Panne, "Deepmimic: Example-guided deep reinforcement learning of physics-based character skills," *ACM Transactions On Graphics (TOG)*, vol. 37, no. 4, pp. 1–14, 2018. [2](#)
- [56] T. He, J. Gao, W. Xiao, Y. Zhang, Z. Wang, J. Wang, Z. Luo, G. He, N. Sobanbab, C. Pan *et al.*, "Asap: Aligning simulation and real-world physics for learning agile humanoid whole-body skills," *arXiv preprint arXiv:2502.01143*, 2025. [2](#)
- [57] X. B. Peng, Z. Ma, P. Abbeel, S. Levine, and A. Kanazawa, "Amp: Adversarial motion priors for stylized physics-based character control," *ACM Transactions on Graphics (ToG)*, vol. 40, no. 4, pp. 1–20, 2021. [2](#)
- [58] X. B. Peng, Y. Guo, L. Halper, S. Levine, and S. Fidler, "Ase: Large-scale reusable adversarial skill embeddings for physically simulated characters," *ACM Transactions On Graphics (TOG)*, vol. 41, no. 4, pp. 1–17, 2022. [2](#)
- [59] Z. Fu, Q. Zhao, Q. Wu, G. Wetzstein, and C. Finn, "Humanplus: Humanoid shadowing and imitation from humans," *arXiv preprint arXiv:2406.10454*, 2024. [2](#)
- [60] M. Loper, N. Mahmood, J. Romero, G. Pons-Moll, and M. J. Black, "Smpl: A skinned multi-person linear model," in *Seminal Graphics Papers: Pushing the Boundaries, Volume 2*, 2023, pp. 851–866. [5](#)
- [61] N. Mahmood, N. Ghorbani, N. F. Troje, G. Pons-Moll, and M. J. Black, "Amass: Archive of motion capture as surface shapes," in *Proceedings of the IEEE/CVF international conference on computer vision*, 2019, pp. 5442–5451. [5](#)